Filaments made from A- and B-type lamins differ in structure and organization

Martin W. Goldberg[1,*], Irm Huttenlauch[2], Christopher J. Hutchison[1] and Reimer Stick[2]

[1]School of Biological and Biomedical Sciences, The University of Durham, South Road, Durham DH1 3LE, UK
[2]Department of Cell Biology, University of Bremen, PO Box 33 04 40, 28334 Bremen, Germany
*Authors for correspondence (e-mail: m.w.goldberg@durham.ac.uk; stick@uni-bremen.de)

Accepted 22 October 2007
Journal of Cell Science 121, 215-225 Published by The Company of Biologists 2008
doi:10.1242/jcs.022020

Summary

Lamins are intermediate filament proteins and the major component of the nuclear lamina. Current views of the lamina are based on the remarkably regular arrangement of lamin LIII in amphibian oocyte nuclei. We have re-examined the LIII lamina and propose a new interpretation of its organization. Rather than consisting of two perpendicular arrays of parallel filaments, we suggest that the oocyte lamina consists of parallel filaments that are interconnected in register to give the impression of a second set of perpendicular filaments. We have also used the oocyte system to investigate the organization of somatic lamins. Currently, it is not feasible to examine the organization of somatic lamins in situ because of their tight association with chromatin. It is also difficult to assemble vertebrate lamin filaments in vitro. Therefore, we have used the oocyte system, where exogenously expressed somatic B-type and A-type lamins assemble into filaments. Expression of B-type lamins induces the formation of intranuclear membranes that are covered by single filament layers. LIII filaments appear identical to the endogenous lamina, whereas lamin B2 assembles into filaments that are organized less precisely. Lamin A induces sheets of thicker filaments on the endogenous lamina and significantly increases the rigidity of the nuclear envelope.

Key words: Nuclear lamina, Lamin filaments, *Xenopus* oocyte, feSEM, Lamin A, B-type lamins

Introduction

The nuclear lamina is a protein meshwork located between the inner nuclear membrane and the peripheral chromatin of metazoan cells. The major structural components of the nuclear lamina, the lamins, are members of the intermediate filament protein family. Targeting of lamins to the inner nuclear membrane depends on the presence of a nuclear localization signal (NLS) and posttranslational lipidation (Mattout et al., 2006; Nigg et al., 1992; Young et al., 2005). Lamins interact with both integral proteins of the inner nuclear membrane and with chromatin-binding proteins (Burke and Stewart, 2002; Gruenbaum et al., 2003).

The nuclear lamina is an essential component of metazoan cells (Harborth et al., 2001). It contributes to mechanical stability of the nuclear envelope and is involved in anchoring nuclear pore complexes (NPCs), in chromatin organization, DNA replication and transcription. The importance of lamin function is highlighted by targeted disruption of the lamins, by genetic analysis and RNAi, as well as by mutations in genes encoding lamins that cause a wide range of heritable human diseases – the laminopathies (Broers et al., 2006; Gruenbaum et al., 2003; Mattout et al., 2006).

Based on their domain structure, two types of lamins, A and B (LmnA and LmnB, hereafter referred to as lamin A and lamin B, respectively), can be distinguished. B-type lamins represent the ancestral lamin type (Stick, 1992). They are permanently isoprenylated and remain closely associated with membranes (Nigg et al., 1992). Vertebrate genomes possess two or three genes encoding different lamin B proteins, of which at least one is expressed in every cell type. A-type lamins are restricted to vertebrates and possess ~100 additional amino acid residues in their tail domain (Gruenbaum et al., 2003). Prenylated prelamin A is converted to lamin A soon after incorporation into the lamina by endoproteolytic processing (Weber et al., 1989). This processing step, in which the isoprene moiety is removed, is essential for the function of lamin A. Failure of lamin A processing leads to severe abnormalities, including Hutchinson-Gilford progeria syndrome in man (Broers et al., 2006; Mattout et al., 2006). The synthesis of A-type lamins is developmentally regulated (Burke and Stewart, 2002). Lamin A is absent in early embryonic cells and appears asynchronously during tissue differentiation.

Nuclear lamins have the tripartite domain organization common to all intermediate filament proteins (Herrmann and Aebi, 2004). A central α-helical domain, able to form coiled-coils, is flanked by a short N-terminal and a large globular C-terminal domain. Lamin assembly in vitro starts with the formation of dimers. In the second assembly step, dimers associate head-to-tail into polar protofilaments. Lamin B of *Caenorhabditis elegans* can assemble into 10-nm filaments (Karabinos et al., 2003). By contrast, vertebrate lamins do not form stable 10-nm filaments in vitro. In further steps of assembly, they aggregate laterally and form thick filament bundles and paracrystalline arrays (Herrmann and Aebi, 2004). Expression of vertebrate A- and B-type lamins in insect cells results in the formation of paracrystals and aggregates with a filamentous substructure, respectively (Klapper et al., 1997).

The nuclear lamina of somatic cells appears as an electron-dense layer interposed between the inner nuclear membrane and the peripheral chromatin. It was termed the ‘fibrous lamina’ (Fawcett, 1966), but individual filaments are not discernible. A clear demonstration that the lamina is formed by filaments has been produced so far only for a single cell type, the amphibian oocyte (Aebi et al., 1986).

Amphibian oocytes are giant cells with nuclei that are approximately 100,000-fold larger volume than somatic nuclei, with chromosomes that are not in contact with the nuclear periphery (Gall et al., 2004). In contrast to somatic cells, the nuclear envelope of amphibian oocytes can easily be isolated free of chromatin and other adhering material. It is therefore ideally suited for ultrastructural analyses of the nuclear lamina. The molecular composition of the amphibian oocyte lamina is particularly simple. Lamin LIII [also known as lamin-L(III) or lamin-B3], a B-type lamin, is the major lamin of the *Xenopus* oocyte (Stick, 1987), in which 10-nm IF-like filaments form a lattice of remarkably regular organization (Aebi et al., 1986). Whether other lamins form filaments of similar morphology and whether the organization of these filaments is similar to that found in the *Xenopus* oocyte lamina is, however, still unclear.

We previously observed that B-type lamins, when overexpressed in oocytes, induce the formation of intranuclear membrane structures that harbour the excess protein (Ralle et al., 2004). By contrast, overexpressed lamin A is targeted to the nuclear envelope, where it associates with the endogenous lamina. In this study, we have determined for the first time the ultrastructure of lamin filaments formed by lamin A and lamin B2 in vivo. We show that applying high-resolution field-emission scanning electron microscopy (feSEM) to the amphibian oocyte expression system is a unique means to analyse the organization of lamin filaments and their assembly into higher-order structures.

Results

To study the ultrastructure of filaments formed by individual lamin proteins, we used *Xenopus* oocytes as an experimental system. First, we examined the endogenous lamina containing lamin LIII. Next, N-terminally epitope-tagged versions of *Xenopus* lamins LIII, B2 and prelamin A were each expressed in oocytes. Nuclear envelopes were subsequently isolated, fixed, critical point dried, coated with a thin film of chromium and then examined by feSEM.

Endogenous lamin LIII forms parallel filaments with regular connections

Fig. 1 shows the nucleoplasmic surface of nuclear envelopes of non-injected oocytes. Lamin filaments cover most of the membrane surface between the NPCs (Fig. 1A). These filaments are formed by lamin LIII, the quantitatively major lamin of *Xenopus* oocytes (Stick, 1988; Stick and Krohne, 1982). They have a diameter of 10.4±1.4 nm, including the metal coat. We are uncertain regarding exactly what the chromium film adds to the dimensions. We estimate that it could add ~3 nm to the filament diameter (see Materials and Methods); however, here we only give dimensions that include the coat. This enables us to make comparisons of diameters of different lamin filaments. In large NPC-free areas, lamin filaments appear as a two-dimensional regular arrangement of square units (Fig. 1C), which favours the idea that the lamina consists of two sets of filaments running at right angles to each other, where the square units represent the crossover points (Aebi et al., 1986). However, Triton-extracted preparations suggest that the NPC-free areas are formed by sets of unidirectional parallel filaments that associate laterally and are joined at regular intervals (Fig. 1D). The orientation of the filaments is indicated in some areas by small arrows in Fig. 1A,D. Individual filaments can be followed in non-extracted preparations at high magnification (Fig. 1B) and can be traced for more than 1 μm. At these magnifications, the lateral inter-connections give the impression of a second set of filaments at right angles to the major filaments because they are repeated in the same position across many filaments. The repeat distance between laterally associated lamin filaments is ~16±1 nm, and the repeat distance between the interconnections is similar, being ~15±1.5 nm – hence the orthogonal appearance. Further examples, where this arrangement is apparent, are shown from the same oocyte (Fig. 1E) and from a different oocyte (Fig. 1F,G) and the arrangement is observed in the multiple oocytes that we have examined. In Fig. 1, the filaments run roughly horizontally, with the cross-connections at right angles. In one example, the parallel lamin filaments separate from each other (arrow in Fig. 1E), with one set changing direction around a NPC. We frequently observe that the presence of NPCs disrupts this highly organized arrangement.

Fig. 2A shows part of the same area as Fig. 1B (the left-hand half). Each filament, running horizontally in the figure, is marked with a large arrow, and some of the clearer cross-connections are marked with small arrows. The interconnections appear to be thinner than the filaments, measuring 6.8±0.9 nm (compared with 10.4±1.4 nm), suggesting that the lamina does not consist of two sets of identical perpendicular filaments (Aebi et al., 1986). Our interpretation of the filaments and cross-connections is superimposed on the same image in Fig. 2B, and an illustration of this is presented in Fig. 2C.

The organizations of lamin LIII and lamin B2 filaments differ

Previous transmission electron microscopy (TEM) analysis demonstrated that exogenous expression of CaaX-containing nuclear proteins such as lamin B2 can induce intranuclear membrane proliferation (Prüfert et al., 2004; Ralle et al., 2004). While TEM analysis of sectioned material is suitable to demonstrate the membrane arrangement (Fig. 3F and Fig. 4D), it does not provide information about the supramolecular organization of the lamin proteins associated with these membranes. We therefore used feSEM to analyse the surface structure of intranuclear membrane arrays induced by overexpression of individual *Xenopus* lamins.

Expression of both lamins LIII and B2 induced assembly of intranuclear membranes (compare Fig. 3A with Fig. 4A) that cover large areas of the nuclear envelope without compromising oocyte viability. Both types of membrane arrays form extensive stacks (Fig. 3F and Fig. 4D), which consist of double-membrane structures, somewhat like the nuclear envelope or endoplasmic reticulum (ER), stacked on top of each other. The ‘lumen’ of these structures is ~40-50 nm wide (similar to the lumens of the nuclear envelope and ER), and the thickness of the electron-dense material between each double-membrane structure is ~8-12 nm, which is consistent with a single layer of lamin filaments. The surfaces of most membrane arrays are covered entirely with lamin filaments but are generally devoid of NPCs (Fig. 3C-E).

The diameter of the lamin LIII filaments on these structures is 11.7±1.2 nm, which is slightly larger than that of the endogenous lamin LIII filaments. Statistically, a two-tailed *t*-test gave a value of 0.03, which indicates a moderately significant difference. However, because the difference is small, we are unsure of its actual biological significance. It could reflect a real difference in the number or arrangement of lamin proteins within the filament, but it could equally reflect difficulties in measuring the diameter of filaments in different situations (i.e. on the inner nuclear membrane versus on the extra membrane structures).

The LIII filaments are organized in a remarkably regular, square lattice arrangement that appears identical to that of the endogenous lamina (Fig. 3C-E). Neighbouring filaments are connected to each other and run parallel in straight lines. After extraction with the non-ionic detergent Triton X-100, the filaments show a particularly pronounced repeat pattern along their axis (Fig. 3D, inset in D). The repeat length after Triton X-100 extraction is ~21±1 nm (Fig. 3D inset arrowheads). However, the same repeat only measures on average 14.7±1.5 nm without detergent extraction. This is very close to the repeat distance between interconnections in the

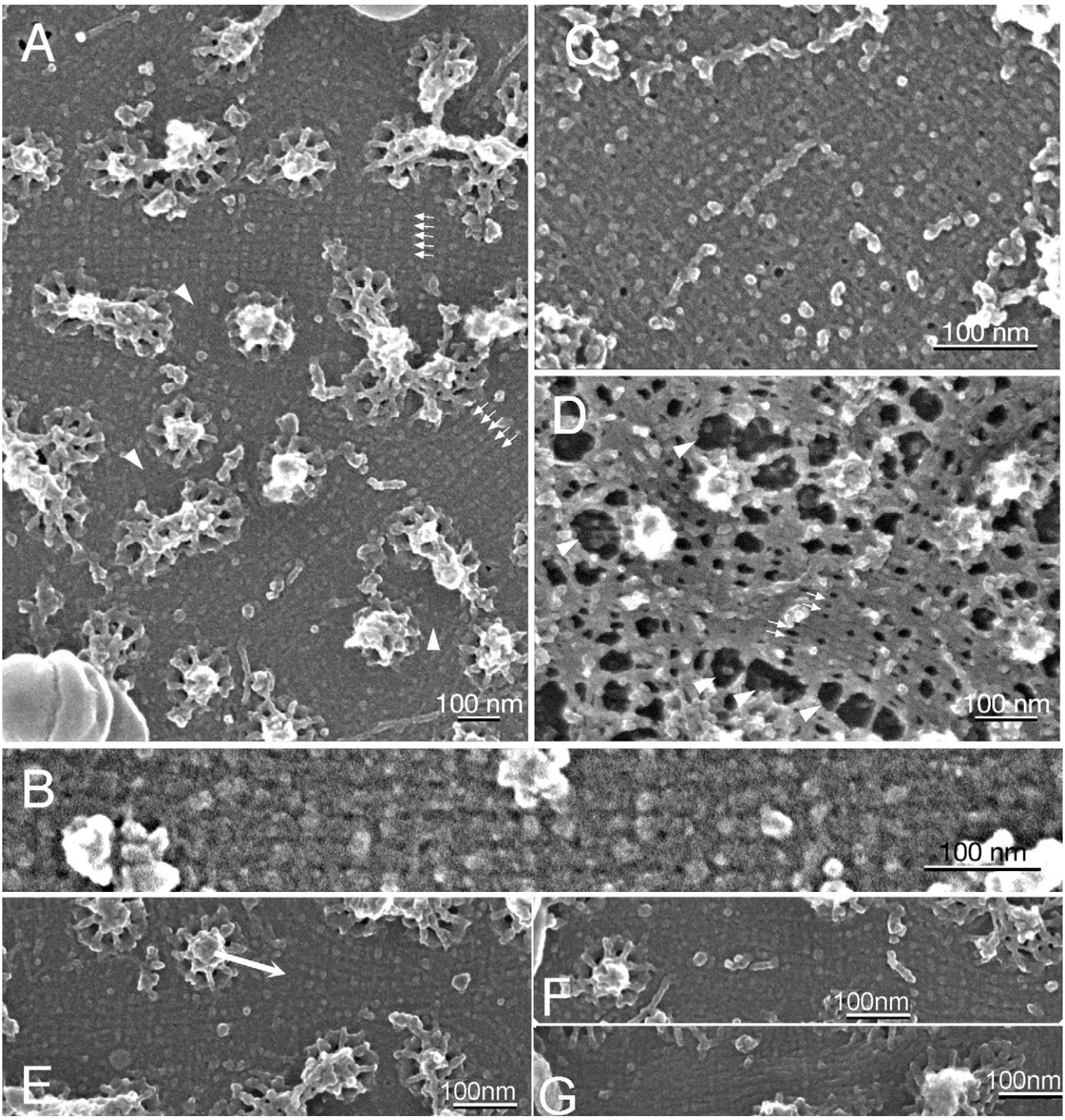

Fig. 1. Field-emission scanning electron microscopy (feSEM) of spreads of non-injected control *Xenopus* nuclear envelopes. (A) Nucleoplasmic face of a nuclear envelope. (B) An area of parallel filaments, indicated by top small horizontal arrows in A is shown at higher magnification. (C) Area of highly ordered lamin lattice at high magnification. (D) Nuclear envelopes treated with 0.5% Triton X-100 before fixation to remove membranes. Some filaments that run in parallel are marked by small arrows. Arrowheads in A and D mark lamin-free membrane areas. (E-G) Further examples, from (E) the same and (F,G) different oocytes, showing arrays of parallel filaments. The arrow in E indicates where one set of parallel filaments bifurcates.

endogenous lamina (15±1.5 nm), suggesting that Triton X-100 causes a relaxation of the structure. Strikingly, LIII filaments are aligned precisely in register with respect to the repeats (Fig. 3D, inset in D), giving rise to the lattice-like appearance (Fig. 3C-E).

Some of the intranuclear membrane arrays are covered only partially with filaments. Such filaments are thinner (8.4±1.1 nm) and are arranged less regularly (Fig. 3B arrows). These regions might represent earlier stages of the formation of the LIII filament network before lateral alignment of the filaments.

To demonstrate that the filaments found on the surface of the membrane arrays are assembled from the overexpressed lamins, we used immunogold labelling in conjunction with feSEM. The excess lamin LIII was distinguishable from the endogenous LIII protein by its FLAG epitope. FLAG-specific antibodies specifically labelled the lamin-induced membrane arrays (Fig. 3G,H). Very few gold particles were found on the endogenous lamina layer, indicating that the excess lamin LIII is incorporated predominantly into filaments on the membrane arrays. Images taken at higher magnification indicate that the immunogold particles are located on the lamin filaments (Fig. 3H).

Expression of lamin B2 induces extensive intranuclear membrane arrays (Fig. 4A) that are densely covered by filaments (Fig. 4B,C). Lamin B2 filaments have an irregular wavy profile and are significantly (as determined by *t*-test) thinner than endogenous and exogenously expressed lamin LIII filaments, measuring ~7.3±0.9 nm in diameter. In areas of apparent low filament density, most B2 filaments run criss-cross with little order, which makes it difficult to follow individual filaments for more than a few hundred nanometres (Fig. 4B). At apparently higher packaging ratios, they often are oriented in one direction (Fig. 4C). Compared with the highly ordered lamin LIII filaments, B2 filaments are less straight, their lateral alignment is less exact and their packaging is less compact (Fig. 4C). Moreover, we never observed B2 filaments organized in the regular lattice-like arrangement that is characteristic for lamin LIII filament networks.

Lamin B2 was labelled either with the lamin B2-specific monoclonal antibody L7-8C6 (Fig. 4E) or with FLAG-epitope-specific antibodies (Fig. 4F). The labelling densities for both LIII and B2 were quantified by counting gold particles and compared with those of non-injected control oocytes, and were approximately 15-20 fold over background. None of the antibodies labelled the outer nuclear envelope in the same preparation. These data show that the excess B-type lamin proteins form filaments on the surface of the intranuclear membranes.

Lamin A filaments

In contrast to B-type lamins, lamin A, when expressed in *Xenopus* oocytes, forms filaments that associate with the endogenous lamina rather than inducing intranuclear membranes (Fig. 5). Expression of lamin A created difficulties with preparing nuclear envelopes for feSEM (see below). Therefore, initially we expressed lamin A at a low level, as indicated by western blots (data not shown) by injecting a smaller amount of plasmid. At low expression levels of lamin A, small filamentous aggregates and short filaments are found between the NPCs where we would normally see the endogenous lamin layer (Fig. 5A, compare with nuclear envelope of uninjected oocyte in Fig. 1A). We therefore presume that these structures form on top of the endogenous lamin layer. Immuno-electron microscopic analysis confirmed the presence of exogenous FLAG-tagged lamin A on top of the endogenous lamina (Fig. 5B). Such labelling was not observed in the uninjected controls. Further examples of short filaments and particles are shown in Fig. 5C,D (arrows). Surprisingly, these short filaments have a significantly larger diameter than the lamins LIII and B2, measuring 16.0±1.7 nm. Sometimes, these structures appear to pile up and form layers in between the NPCs. Such a layered structure, indicated by the large arrows in Fig. 5D, is surrounded by NPCs (arrowheads) that are partially obscured by this layered structure, which shows that the lamin A layer

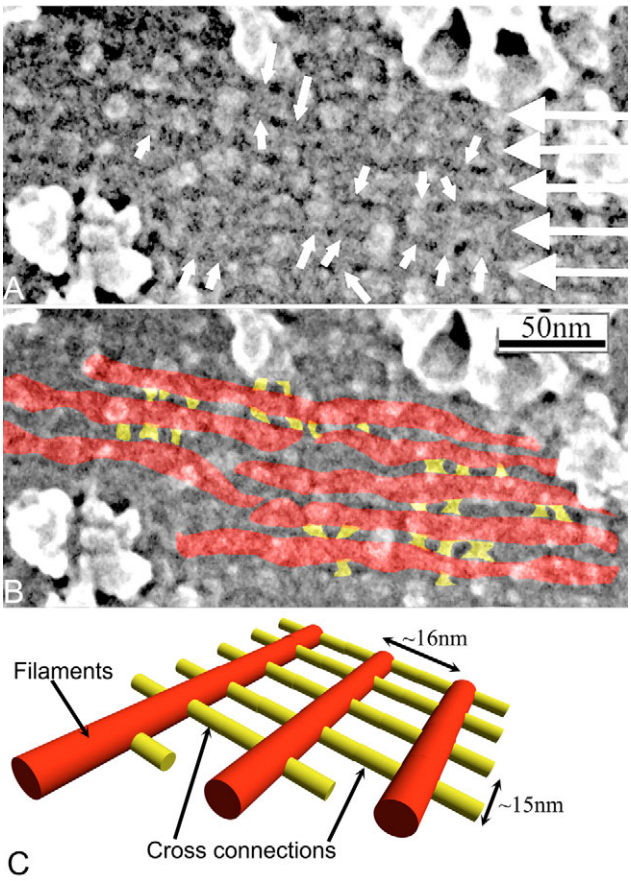

Fig. 2. (A) Same area as Fig. 1B showing the position of parallel filaments (large arrows) and cross-connections (small arrows). (B) our interpretation of the filament and cross-connection arrangement, with filaments coloured red and cross-connections yellow. (C) Proposed model for the arrangement of lamin LIII filaments.

Fig. 3. feSEM and TEM of lamin LIII-induced intranuclear membrane arrays. FLAG-tagged lamin LIII was expressed by nuclear injection of plasmid DNA. (A) Nuclear envelope of an oocyte overexpressing lamin LIII, shown at low magnification. Lamin-induced intranuclear membrane arrays (arrows) are distributed throughout the nuclear envelope. (B) Lamin LIII-induced membrane arrays sparsely covered by lamin filaments. Arrows mark filament-free areas of the extra membrane. (C-E) Lamin LIII-induced membrane arrays densely packed with filaments. Nuclear envelopes were either (C) fixed immediately or (D,E) treated with 0.5% Triton X-100 before fixation to remove membranes. In several areas of the membrane arrays, the LIII filaments are organized in a lattice-like arrangement. Note the pronounced repeat pattern along the LIII filament axis in D. The inset in D shows repeats at higher magnification. The line of arrowheads in the inset highlights the repeats. (F) TEM section of an isolated oocyte nucleus expressing lamin LIII. (G,H) Immuno-feSEM detection of FLAG-tagged lamin LIII on intranuclear membrane arrays using FLAG-specific antibodies. The immuno-gold labels are indicated by gold spots in G and H.

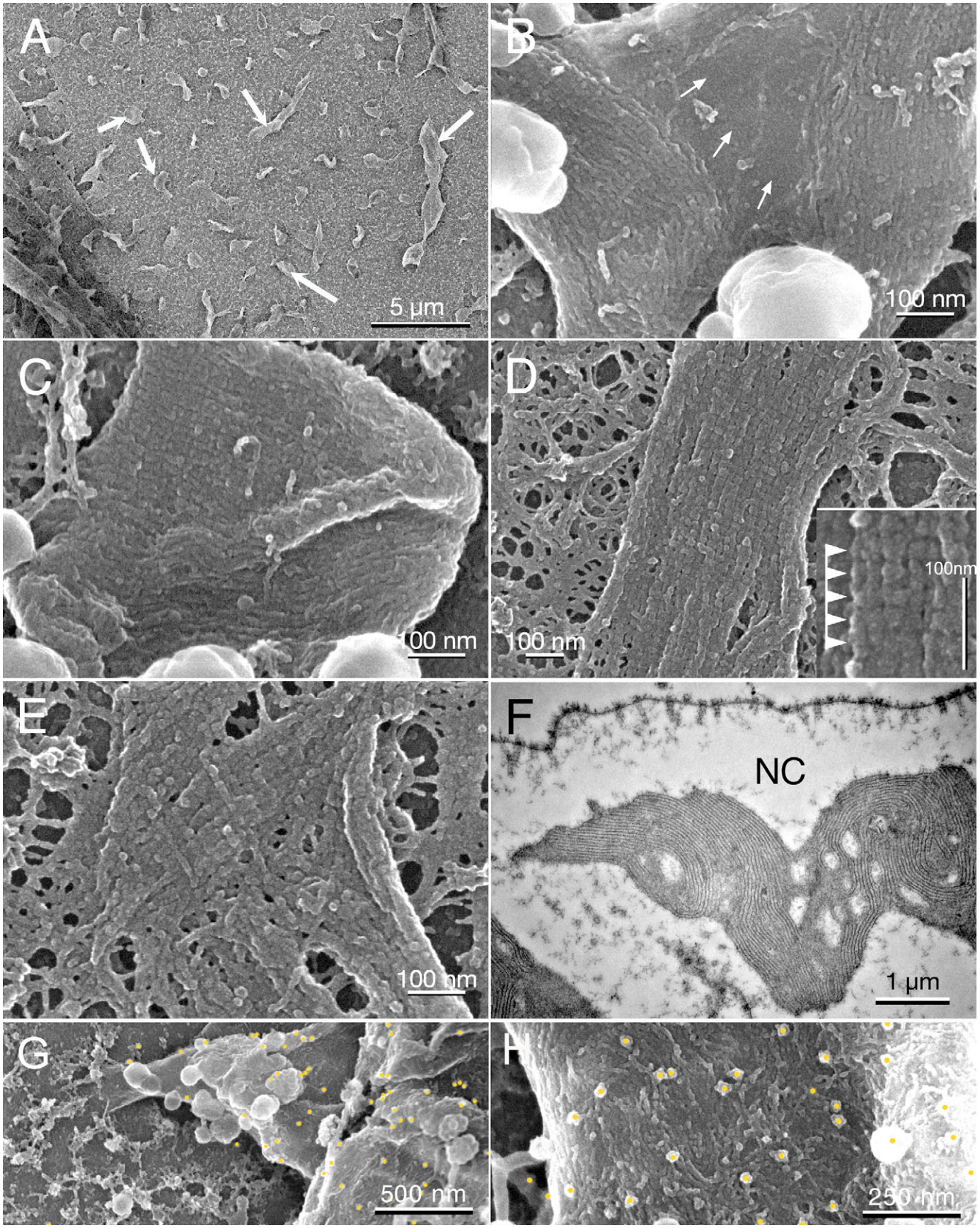

Fig. 3. See previous page for legend.

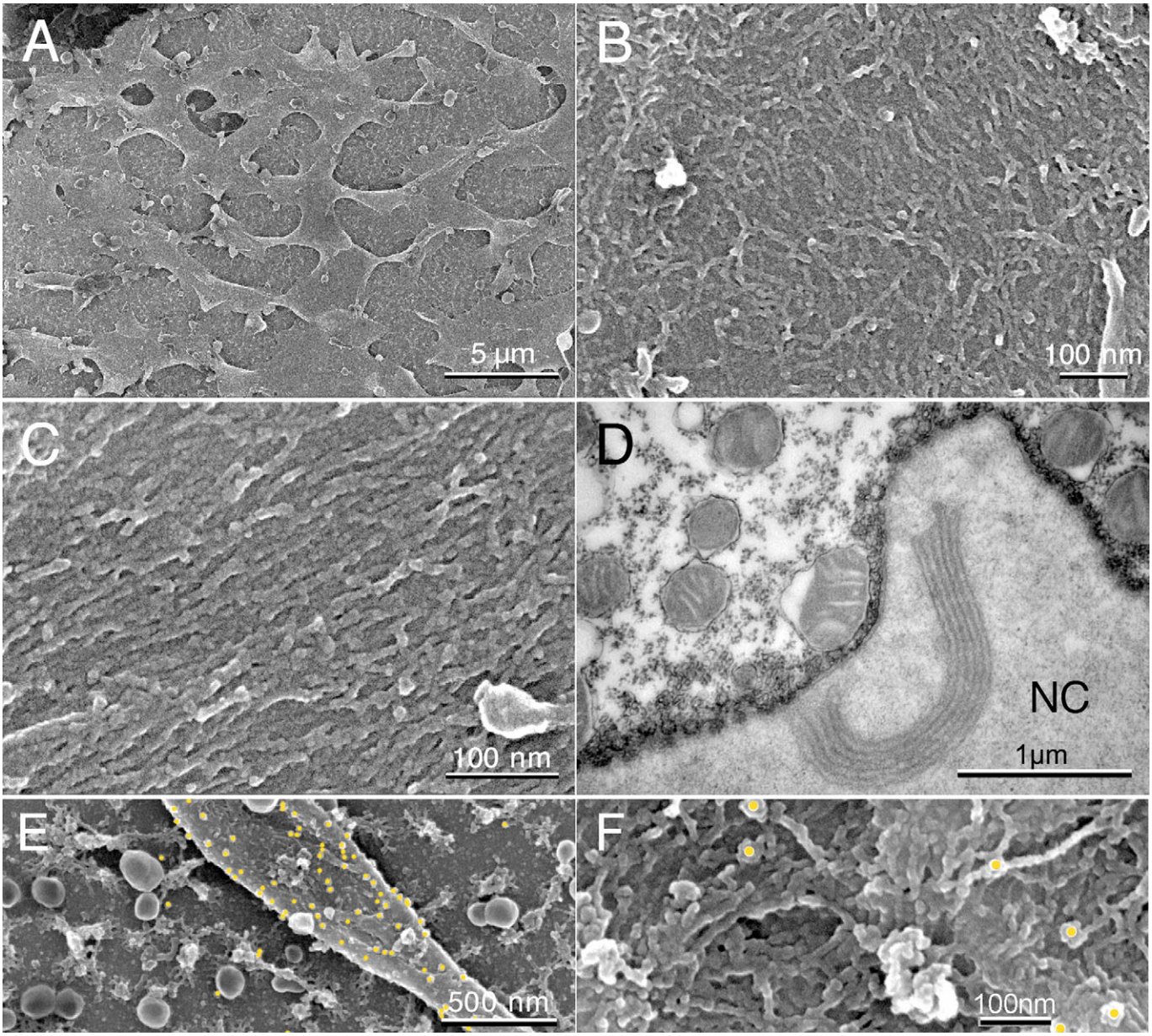

Fig. 4. feSEM and TEM of lamin B2-induced intranuclear membrane arrays. FLAG-tagged lamin B2 was expressed by nuclear injection of plasmid DNA. (A) Nuclear envelope of an oocyte overexpressing lamin B2, shown at low magnification. (B) Membrane arrays covered by irregular wavy lamin B2 filaments. (C) A more-ordered package of lamin B2 filaments on a membrane array. Note the more-or-less parallel alignment of B2 filaments. (D) TEM section of an isolated oocyte nucleus expressing lamin B2. (E,F) Immuno-feSEM detection of lamin B2 on membrane arrays using the mAb L7-8C6 that is specific for *Xenopus* lamin B2 (E) and antibodies against the FLAG epitope (F). The immuno-gold labels are indicated by gold spots in E and F.

builds up to a significant thickness relative to NPC height, as shown in stereo pairs (Fig. 5E).

Nuclei of oocytes that expressed lamin A at higher levels (by injection of a higher concentration of plasmid and confirmed on western blots; data not shown) are stiff and resistant to deformation and could not be processed for feSEM in the same way as oocytes expressing B-type lamins or controls. When pushed down forcefully onto a chip by a pipette tip, they do not adhere to the chip but round up again upon release of the mechanical force. As it was impossible to mount nuclear envelopes of these rigid nuclei onto chips, they were isolated and processed in solution. Images of the inner surface of these nuclear envelopes were difficult to interpret owing to the multiple layers of lamin A filaments that cover the entire area of the endogenous nuclear lamina (Fig. 6A,B). Individual filaments, however, can be distinguished clearly at many sites (Fig. 6A,B small arrows). These lamin A filaments, like the short filaments, are significantly thicker than LIII and B2 filaments and measure 15.7±2.0 nm in diameter, which is not significantly different to the diameter of the shorter structures observed after low-level expression of lamin A. We therefore propose that these consist of the same substructural components.

The repeat pattern found in lamin A filaments is less obvious than that of LIII filaments. Lamin A filaments run in tight bundles

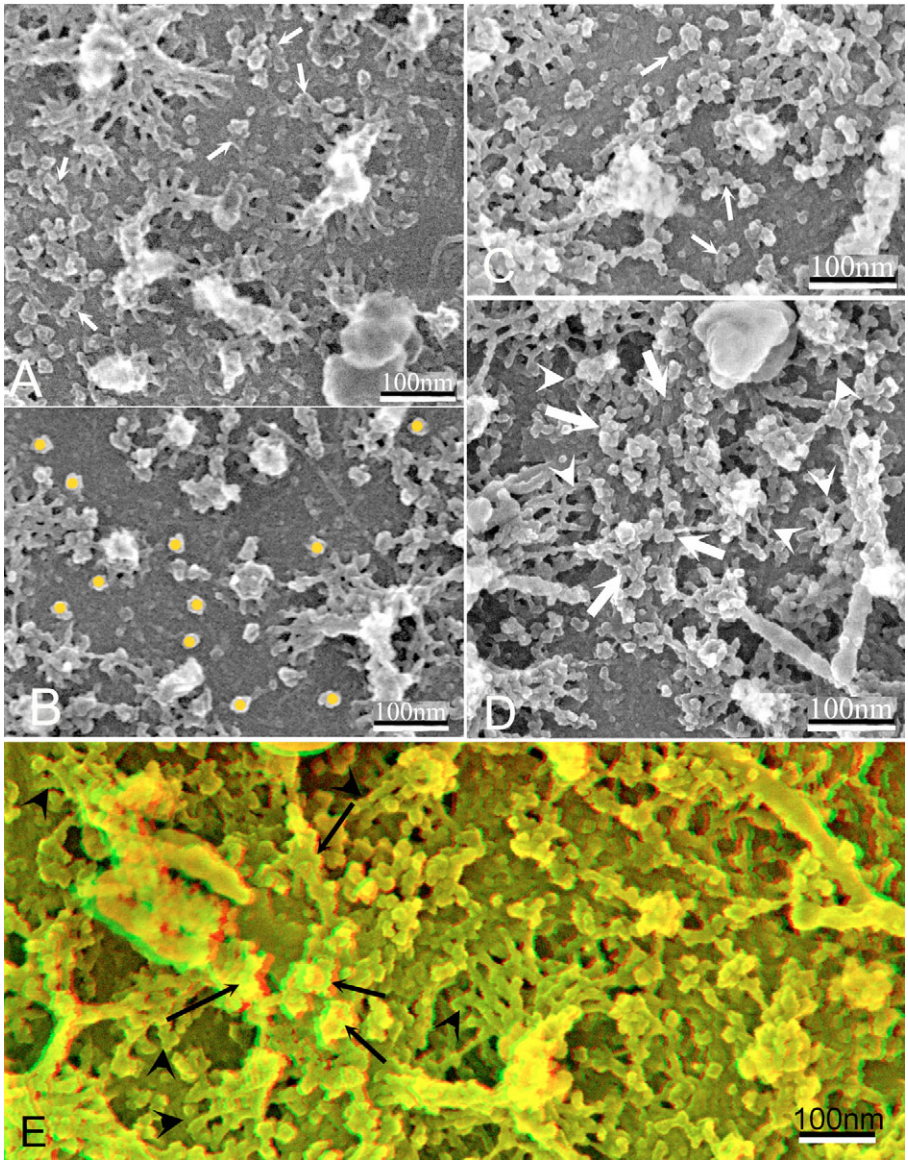

Fig. 5. feSEM of nuclear envelope spreads of oocytes expressing lamin A. FLAG-tagged lamin A was expressed by nuclear injection of a small amount (0.38 ng) of plasmid DNA. (A-C) Small filamentous aggregates are marked by arrows in A and C, and immuno-gold labels against FLAG are indicated by gold spots in B. (D,E) NPC baskets are indicated by arrowheads in D, and a multilayer filament region is indicated by large arrows in D and E. Image E is a red-green 3D stereo pair of an area similar to that in D and requires red-green glasses.

that surround the NPCs and tend to pile up on top of each other. They appear to form multilayered sheets of variable thickness such that NPC baskets (Fig. 6A,B large arrows) are completely surrounded by lamin A filaments – quite different from the membrane-associated thin layers formed by B-type lamins. We have deduced that the structures in Fig. 6A,B (large arrows) are NPC baskets because: their size is consistent with the distal basket ring; in some cases, basket filaments are seen (arrowheads); and the lamin filaments appear to be inhibited from assembling through or over these structures, which is consistent with the gaps in the lamina observed in thin sections by TEM (see below; Fig. 6D).

In TEM cross-sections of control nuclei, the lamina (consisting of a single layer of predominantly lamin LIII) is barely discernible (Fig. 6C). Expression of lamin A results in considerable thickening of the lamin layer (Fig. 6D). Lamin A filament bundles appear, in thin sections, as compact electron-dense material attached to the endogenous lamina (Fig. 6D). The experimentally induced lamin A layers bear remarkable resemblance to thick laminae found in particular somatic cells (Fawcett, 1966; Ghadially, 1988; Höger et al., 1991; Kalifat et al., 1967; Patrizi and Poger, 1967; Stick, 1987). At the position of NPCs, the lamin A layer is interrupted (Fig. 6D arrows). This is consistent with the en face views seen by feSEM (Fig. 6A,B large arrows).

Discussion

We have re-examined the structural organization of the lamina in *Xenopus* oocytes using high-resolution chromium coating and feSEM. From the resulting images, we propose to modify the original model based on TEM images of detergent-extracted, platinum-shadowed nuclear envelopes (Aebi et al., 1986). The generally accepted view is that the lamina consists of two sets of parallel filaments arranged at right angles to each other. Although this view is based solely on images from *Xenopus* oocytes, whose predominant lamin is the oocyte-specific LIII protein, it is often presumed that other lamins might form similar structures. We show here that not only does the LIII lamina probably consist of a single set of parallel filaments with distinct regular cross-connections, but other lamins, especially A-type lamins, form different structures.

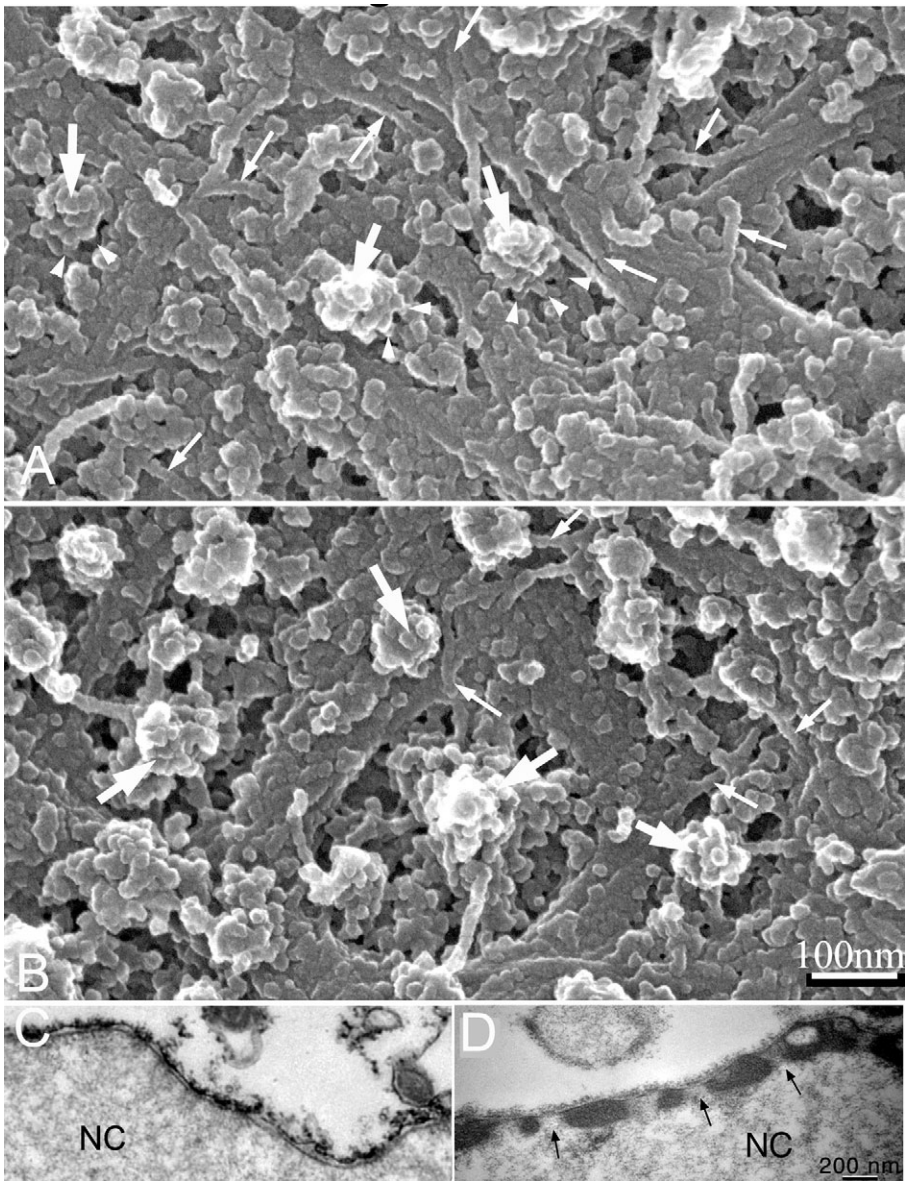

Fig. 6. FeSEM of isolated nuclear envelopes from oocytes expressing high levels of lamin A after injection of 1.5 ng of plasmid DNA. (A,B) Lamin A filaments that are arranged in layered bundles are indicated by small arrows; they surround, but appear not to interact with, structures that are consistent with NPC baskets. In general, the distal basket ring is visible (large arrows), and sometimes basket filaments can be seen (arrowheads). Oocytes expressing lamin A were also analysed by TEM thin sections and compared with controls. (C,D) The lamina is hardly discernible in (C) controls but forms a thick electron-dense layer in (D) oocytes expressing lamin A, which leaves the NPCs clear (arrows).

Lamin LIII forms arrays of parallel fibers with regular cross-connections

By the use of a brief low-salt wash, fixation with tannic acid in addition to glutaraldehyde and then coating with an essentially grainless chromium coat, we have been able to visualize details of the endogenous lamin LIII lamina in *Xenopus* oocytes without detergent extraction. Initial examination of these images gives an impression of an orthogonal array of filaments, as previously suggested (Aebi et al., 1986), and indeed we see repeat distances of 15-16 nm in both vertical and horizontal directions. However, closer examination reveals that the filaments in one direction appear dominant over the other, and measurements show that these are significantly thicker. We are also able to follow the thicker filaments for considerable distances, whereas the structures perpendicular to them are much harder to follow. These images suggest that this lamina does not consist of two sets of identical perpendicular filaments but, rather, a single set of parallel filaments that associate laterally with each other by regularly spaced, in-register, cross-connections, giving the appearance of a second set of filaments. Significantly, close inspection of the images published by Aebi and colleagues (Aebi et al., 1986) can be interpreted in the same way. It is unclear how either an orthogonal array (Aebi et al., 1986) or the organization proposed here could be assembled from lamin proteins because neither structure has been reconstituted in vitro (for a review, see Herrmann and Aebi, 2004). However, when lamins are assembled in vitro, they form structures such as beaded filaments and paracrystals with 24-25 nm repeats (Aebi et al., 1986; Foeger et al., 2006; Heitlinger et al., 1991). Such structures are consistent with a lateral association of head-to-tail lamin fibers. Such an arrangement is more similar to the organization proposed here than to perpendicularly organized filaments. We do not know whether the parallel filaments or cross-connections consist entirely of lamins or whether other proteins are involved in this structure. Such a question can be answered, however, by immunogold labelling with antibodies to known lamin-interacting proteins. Because we can reconstitute the assembly of lamin LIII into similar structures on intranuclear membranes by

overexpression of the protein (discussed below), we can also analyse how mutations have specific effects on the organization.

B-type lamins

We speculate that the inability of lamins to form in vitro two-dimensional arrays is due to the lack of a membrane surface on which to assemble. In addition, it has proved impossible so far to access somatic lamins in situ for structural analysis owing to the tight association of chromatin and other intranuclear structures. Therefore, we have taken the approach of expressing somatic lamins in *Xenopus* oocytes, where the inner nuclear membrane is easily accessible. In the case of B-type lamins, exogenous expression induces the formation of membrane surfaces on which lamin arrays assemble and that can be studied by feSEM. To check for the correct assembly of lamins in this system, we first overexpressed lamin LIII, which formed filament arrays that appeared to be identical to the endogenous lamina in oocytes.

The results show that the morphologies of lamin LIII and B2 filaments are different (compare Fig. 3 with Fig. 4). Statistically, LIII filaments appear thicker (Fig. 7, chart). They align laterally and in register, forming extensive filament layers of lattice-like appearance that are very similar to the regular arrangement of the endogenous oocyte lamina. Lamin B2 filaments are thinner, less regular and do not form regularly ordered lattice-like layers. This suggests that the arrangement in regular layers is specific for lamin LIII rather than being a general feature of lamin filaments. Alternatively, the organization in lattice-like layers might be dependent on an additional factor(s) that itself is specific for particular lamins. However, such factors might still be present in oocytes and recruited by lamin B2. For instance, preliminary data suggest that Xp57 (the lamin B receptor) relocates from the ER to the nucleus upon expression of exogenous lamin B2 (our unpublished data). We have not yet investigated whether this is true for other lamin-interacting factors.

Regular lamin LIII layers on the surface of the extra membranes extend over much larger areas than those found in the endogenous lamina. This suggests that the number of interspersed NPCs limits the dimensions of regularly arranged filament layers in the endogenous oocyte lamina.

In TEM thin-sections, the lamina appears as a more or less homogenous layer, in which filaments are not discernible. One currently insurmountable obstacle to analyse the ultrastructure of laminae of somatic cells is their association with chromatin. Ultrastructural analysis on nuclear ghosts that were stripped of chromatin (Dwyer and Blobel, 1976) did not achieve high resolution because the preparation involved a harsh treatment. An early SEM study of the cytoplasmic side of detergent-treated mouse liver nuclei also did not reveal the filamentous nature of the lamina (Kirschner et al., 1977). Amphibian oocytes are particularly suitable for structural analyses as their chromosomes are not bound to the nuclear periphery, meaning that nuclear envelopes free of nucleoplasmic material can be prepared. This is one of the reasons why the current view of the structure of the nuclear lamina is nearly exclusively based on images showing the regular organization of the *Xenopus* oocyte lamina (Aebi et al., 1986; Stewart and Whytock, 1988). It is also why we have chosen this system as the only way we know to approach gaining an understanding of the organization of the somatic lamins. Although it might not give a complete picture because of the lack of chromatin association and possibly other interacting factors that are specific to somatic cells, it does assemble recognizable lamin filaments, which, in the case of lamin LIII at least, recapitulate the known structural organization. It will also be possible in the future to coexpress known interacting proteins that are not present in oocytes and even introduce chromatin.

Based on measurements of the elastic properties of *Xenopus* oocyte nuclear envelopes, it has been proposed that the oocyte lamina is compressed in its native state and that it expands upon

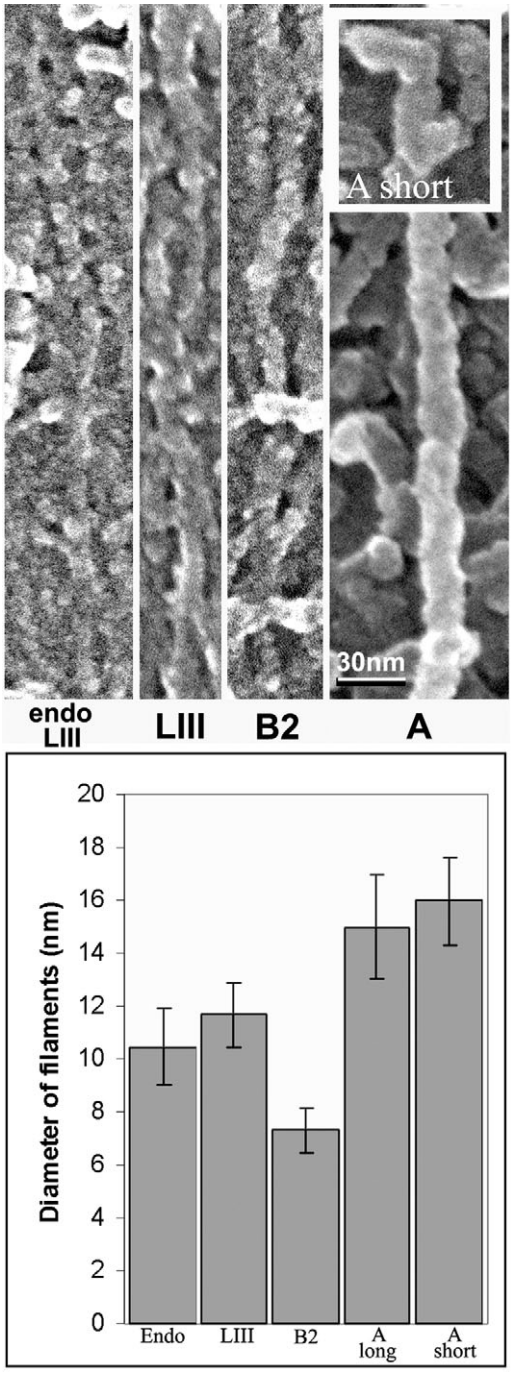

Fig. 7. Comparison of filaments formed by endogenous LIII ('endo LIII'), overexpressed LIII, lamin B2 and lamin A, and short filaments of lamin A obtained at low levels of expression ('short A'; inset). All filaments are shown at the same magnification. The chart shows the mean diameter, including the chromium coat, with standard deviation bars for each filament type (n>100).

swelling to the flat orthogonal network seen by TEM (Dahl et al., 2004). Our data show that LIII lamin filaments are indeed tightly packed and highly organized but that this particular arrangement is not found for the somatic B-type lamins, at least when expressed in oocytes. Another model, also deduced from measurements of the elastic properties of nuclear envelopes, describes the lamina as a heterogeneous meshwork consisting of both regular lattice domains and interconnecting filaments (Rowat et al., 2005). This description matches closely the lamin filament distribution described herein. Whether the latter model, which was proposed to explain data obtained on somatic cell nuclei that express lamin A, might be applicable to *Xenopus* oocytes has yet to be established.

Lamin A

In somatic cells, the thickness of the lamin layer varies greatly between different cell types and might change depending on the physiological or pathological state (Ghadially, 1988). The relationship between the thickness of a particular lamina and its molecular composition is, however, not clear. Coexpression of A-type and B-type lamins within the same cell has been described in a multitude of reports. Differences in expression patterns and membrane-association properties between A-type and B-type lamins suggest different roles with respect to lamina architecture and function (Delbarre et al., 2006). B-type lamins are permanently isoprenylated and are closely associated with membranes. By contrast, possible lipid-mediated interactions of prelamin A with membranes are abolished by the endoproteolytic processing to mature lamin A that removes the isoprene moiety (Mattout et al., 2006; Young et al., 2005). Importantly, this processing machinery is also active in *Xenopus* oocytes (Annette Peter and R.S., unpublished), and a significant fraction of pre-lamin A expressed here is processed into mature lamin A.

Here, we show that, upon expression in oocytes, lamin A forms filaments that associate with the endogenous lamina. Lamin A filaments appear to be different from B-type lamin filaments, possessing a wider diameter (Fig. 7). They form a compact layer that covers the entire nuclear lamina but leaves the regions of the NPCs free. The appearance of the lamin-A-containing nuclear envelopes in TEM cross-sections appears to be similar to that of somatic cells, with particularly thick nuclear laminae. Unlike somatic cells, however, chromatin is not associated with the oocyte nuclear lamina. Our observations suggest a plausible way for how cells could change the thickness of their lamina by regulating the level of lamin A expression in response to physiological clues or during differentiation.

Remarkably, the mechanical properties of oocyte nuclei change parallel with the expression level of lamin A. Compared with control nuclei or nuclei overexpressing B-type lamins, nuclei that contain large amounts of lamin A filaments are much stiffer and resist deformation to an extremely high degree. Somatic cell nuclei are filled with chromatin, and this solid compound significantly contributes to the mechanical stability of these nuclei. The oocyte nuclear content is a liquid protein solution, rather than a solid compound, and cannot provide mechanical stability to these nuclei. Experiments with the actin-specific nuclear export factor Exp6 have provided evidence that the intranuclear actin network represents the major stabilizing element of amphibian oocyte nuclei (Bohnsack et al., 2006). The same authors postulate the plausible argument that only a small fraction of the mechanical support might originate from the single-layered lattice of the endogenous oocyte lamina. Our results show that expression of lamin A, which is normally absent from oocytes, can significantly increase the mechanical stability of these nuclei. As the contribution of chromatin is negligible in oocyte nuclei and as the effect of nuclear actin can be abrogated experimentally (Bohnsack et al., 2006), our experimental system is well suited to quantify the contribution of lamin A filaments to the mechanical properties of nuclear envelopes.

Concluding remarks

Here, we have demonstrated that different lamin proteins form into distinctive individual filaments with characteristic organizations. B-type lamins form thin, highly organized layers that are closely associated with membranes, whereas lamin A forms thick bundles and layers on top, which add to the mechanical rigidity, of the nuclear envelope. Mutations in the gene encoding lamin A cause numerous human diseases, including Emery-Dreyfus muscular dystrophy and the premature aging disease Hutchinson-Gilford progeria syndrome (Broers et al., 2006; Mattout et al., 2006). At the cellular level, expression of mutant lamin A results in a severe alteration in nuclear morphology and changes in the mechanical properties of the nucleus (Dahl et al., 2004; Goldman et al., 2004). The oocyte experimental system that we have established and described here is well suited to study lamin organization and the ability of mutant lamins to form and organize filaments. Moreover, use of techniques such as atomic force microscopy can now be used to determine and to analyse how the contribution of these proteins affects the mechanical properties of the nuclear envelope and how these properties change in the presence of dominant lamin A mutant proteins. The structures that we observe involving somatic lamins will lack many of their normal interactions with intranuclear and nuclear envelope structures, which could influence the organization. However, because these lamin structures are assembled onto intranuclear membranes, they are likely to be the structures that most closely resemble in situ laminae, which have so far proved impossible to access for structural analysis.

Materials and Methods

Oocyte isolation and microinjection

Female *Xenopus laevis* (Daudin) were purchased from NASCO (USA). Oocytes were surgically removed and were defolliculated by collagenase treatment, as described previously (Sive et al., 2000). Plasmid DNA (27.5 to 110 ng/μl in H_2O) was injected into the oocyte nucleus (13.8 nl per nucleus) with a Nanoliter-Injector (World Precision Instruments). DNA was mixed with Blue Dextran (10 mg/ml final concentration) (Fluka) to confirm successful nuclear injection. Synthetic RNA (440 ng/μl in H_2O) was injected into the cytoplasm of oocytes (13.8 to 27.6 nl per oocyte). Injected oocytes were incubated for 16 to 24 hours at 18°C to allow expression of lamin proteins. The construction of FLAG-epitope-tagged *Xenopus laevis* lamins LIII, B2 and prelamin A has been described previously (Hofemeister et al., 2000; Ralle et al., 2004).

Preparation of nuclei and nuclear envelopes for feSEM and TEM

The preparation of nuclear envelopes and processing for feSEM was as described previously (Goldberg and Allen, 1992). To remove membrane lipids from the spread nuclear envelopes, an additional wash for 5 minutes in 0.5% Triton in 5:1 buffer was included before fixation. Specimens were viewed in a Hitachi Model 5200 field emission scanning electron microscope at 30kV accelerating voltage.

Nuclear envelopes of oocytes expressing lamin A that did not attach to silicon chips were isolated in 5:1 buffer containing 10 mM $MgCl_2$. They were sucked up and down in a narrow-bore pipette until they broke up and released their gelified nuclear content. For fixation and dehydration, the isolated nuclear envelopes were transferred by a pipette. For transfer into the critical point dryer, they were enveloped in a lens cleaning paper under ethanol. After critical point drying, they were mounted onto silicon chips with electrical conductive tape (Agar). Oocyte nuclei were processed for TEM as described previously (Goldberg and Allen, 1992). Thin-sections were viewed in a Hitachi H7600 TEM at 100 kV.

Antibodies and preparation of samples for immuno-feSEM

A polyclonal rabbit antibody (catalogue number F-7425, Sigma) and the mouse monoclonal antibody (mAb) M2 (catalogue number F-3165, Sigma), directed against the FLAG epitope, were used both at 20 μg/ml IgG for immunogold labelling. mAb L7-8C6, directed against *Xenopus* lamin B2 has been described previously (Stick, 1988). For immuno-feSEM, silicon chips with attached nuclear envelopes were transferred to a Petri dish containing 2% formaldehyde in 100 mM HEPES-KOH, pH 7.4 and were fixed for 10 minutes at room temperature. They were then briefly washed in PBS (140 mM NaCl, 2.7 mM KCl, 8.1 mM Na_2HPO_4, 1.5 mM KH_2PO_4, pH 7.3), washed for 10 minutes in 100 mM glycine in PBS and for 1 hour in 1% fish gelatine (Sigma) in PBS and were incubated for 1 hour with primary antibodies against the FLAG epitope or lamin B2 (ascites fluid diluted 1:125). Primary antibodies were removed by washing for 30 minutes with several changes in PBS, and samples were incubated for 1 hour with 10-nm gold-conjugated secondary goat anti-rabbit antibody (polyclonal anti-FLAG antibody) or goat anti-mouse antibody (mAbs M2 and L7-8C6) (Amersham; catalogue numbers RPN421 and RPN431, respectively). Secondary antibodies were removed as described above. Samples were then post-fixed with 2% glutaraldehyde, 0.2% tannic acid in 100 mM HEPES-KOH, pH 7.4 and processed for feSEM as described above. Colloidal gold particles were visualized using a solid-state backscatter electron detector.

Measurements of digital images

Measurements were acquired with the image software ImageJ (Abramoff et al., 2004) and Image Pro Plus (Media Cybernetics). At least 100 measurements were taken for each filament type. Although we can estimate the contribution of the metal coating to the diameter of the filaments, this is difficult. Uncoated lamin filaments are difficult to make out and to measure accurately. NPC basket filaments can be measured but are variable in diameter and vary along their length, so measurements are still open to interpretation. We found that the thickness of chromium used in this study adds approximately 2.5 nm to the basket filament diameter, but preliminary data suggest that uncoated endogenous lamin LIII filaments might be ~6-7 nm, which would suggest a chromium thickness of 3-4 nm, but these are based only on limited measurements. Because there remains some uncertainty, we quote measurements that include the chromium coat and use them for comparison of filaments assembled from different lamins and substructures, rather than considering them as being absolute measurements.

We thank Emmajane Newton and Christine Richardson for help with the electron microscopy, David Hyde for preparation of injection needles, and Pamela Ritchie for technical support. This work was supported by grants from the Deutsche Forschungs Gemeinschaft to R.S. (Sti 98/7-1) and the Wellcome Trust to M.W.G. (Grant Number 065860).

References

Abramoff, M. D., Magelhaes, P. J. and Ram, S. J. (2004). Image processing with ImageJ. *Biophoton. Int.* **11**, 36-42.

Aebi, U., Cohn, J., Buhle, L. and Gerace, L. (1986). The nuclear lamina is a meshwork of intermediate-type filaments. *Nature* **323**, 560-564.

Bohnsack, M. T., Stuven, T., Kuhn, C., Cordes, V. C. and Görlich, D. (2006). A selective block of nuclear actin export stabilizes the giant nuclei of *Xenopus* oocytes. *Nat. Cell Biol.* **8**, 257-263.

Broers, J. L., Ramaekers, F. C., Bonne, G., Yaou, R. B. and Hutchison, C. J. (2006). Nuclear lamins: laminopathies and their role in premature ageing. *Physiol. Rev.* **86**, 967-1008.

Burke, B. and Stewart, C. L. (2002). Life at the edge: the nuclear envelope and human disease. *Nat. Rev. Mol. Cell Biol.* **3**, 575-585.

Dahl, K. N., Kahn, S. M., Wilson, K. L. and Discher, D. E. (2004). The nuclear envelope lamina network has elasticity and a compressibility limit suggestive of a molecular shock absorber. *J. Cell Sci.* **117**, 4779-4786.

Delbarre, E., Tramier, M., Coppey-Moisan, M., Gaillard, C., Courvalin, J. C. and Buendia, B. (2006). The truncated prelamin A in Hutchinson-Gilford progeria syndrome alters segregation of A-type and B-type lamin homopolymers. *Hum. Mol. Genet.* **15**, 1113-1122.

Dwyer, N. and Blobel, G. (1976). A modified procedure for the isolation of a pore complex-lamina fraction from rat liver nuclei. *J. Cell Biol.* **70**, 581-591.

Fawcett, D. W. (1966). On the occurrence of a fibrous lamina on the inner aspect of the nuclear envelope in certain cells of vertebrates. *Am. J. Anat.* **119**, 129-145.

Foeger, N., Wiesel, N., Lotsch, D., Mucke, N., Kreplak, L., Aebi, U., Gruenbaum, Y. and Herrmann, H. (2006). Solubility properties and specific assembly pathways of the B-type lamin from Caenorhabditis elegans. *J. Struct. Biol.* **155**, 340-350.

Gall, J. G., Wu, Z., Murphy, C. and Gao, H. (2004). Structure in the amphibian germinal vesicle. *Exp. Cell Res.* **296**, 28-34.

Ghadially, F. N. (1988). *Ultrastructural Pathology of the Cell and Matrix*. London: Butterworths.

Goldberg, M. W. and Allen, T. D. (1992). High resolution scanning electron microscopy of the nuclear envelope: demonstration of a new, regular, fibrous lattice attached to the baskets of the nucleoplasmic face of the nuclear pores. *J. Cell Biol.* **119**, 1429-1440.

Goldman, R. D., Shumaker, D. K., Erdos, M. R., Eriksson, M., Goldman, A. E., Gordon, L. B., Gruenbaum, Y., Khuon, S., Mendez, M., Varga, R. et al. (2004). Accumulation of mutant lamin A causes progressive changes in nuclear architecture in Hutchinson-Gilford progeria syndrome. *Proc. Natl. Acad. Sci. USA* **101**, 8963-8968.

Gruenbaum, Y., Goldman, R. D., Meyuhas, R., Mills, E., Margalit, A., Fridkin, A., Dayani, Y., Prokocimer, M. and Enosh, A. (2003). The nuclear lamina and its functions in the nucleus. *Int. Rev. Cytol.* **226**, 1-62.

Harborth, J., Elbashir, S. M., Bechert, K., Tuschl, T. and Weber, K. (2001). Identification of essential genes in cultured mammalian cells using small interfering RNAs. *J. Cell Sci.* **114**, 4557-4565.

Heitlinger, E., Peter, M., Haner, M., Lustig, A., Aebi, U. and Nigg, E. A. (1991). Expression of chicken lamin B2 in Escherichia coli: characterization of its structure, assembly, and molecular interactions. *J. Cell Biol.* **113**, 485-495.

Herrmann, H. and Aebi, U. (2004). Intermediate filaments: molecular structure, assembly mechanism, and integration into functionally distinct intracellular Scaffolds. *Annu. Rev. Biochem.* **73**, 749-789.

Hofemeister, H., Weber, K. and Stick, R. (2000). Association of prenylated proteins with the plasma membrane and the inner nuclear membrane is mediated by the same membrane-targeting motifs. *Mol. Biol. Cell* **11**, 3233-3246.

Höger, T. H., Grund, C., Franke, W. W. and Krohne, G. (1991). Immunolocalization of lamins in the thick nuclear lamina of human synovial cells. *Eur. J. Cell Biol.* **54**, 150-156.

Kalifat, S. R., Bouteille, M. and Delarue, J. (1967). Etude ultrastructurale de la lamelle dense observee au contact de la membrane nucleaire interne. *J. Microsc. Paris* **6**, 1019-1026.

Karabinos, A., Schunemann, J., Meyer, M., Aebi, U. and Weber, K. (2003). The single nuclear lamin of *Caenorhabditis elegans* forms in vitro stable intermediate filaments and paracrystals with a reduced axial periodicity. *J. Mol. Biol.* **325**, 241-247.

Kirschner, R. H., Rusli, M. and Martin, T. E. (1977). Characterization of the nuclear envelope, pore complexes, and dense lamina of mouse liver nuclei by high resolution scanning electron microscopy. *J. Cell Biol.* **72**, 118-132.

Klapper, M., Exner, K., Kempf, A., Gehrig, C., Stuurman, N., Fisher, P. A. and Krohne, G. (1997). Assembly of A- and B-type lamins studied in vivo with the baculovirus system. *J. Cell Sci.* **110**, 2519-2532.

Mattout, A., Dechat, T., Adam, S. A., Goldman, R. D. and Gruenbaum, Y. (2006). Nuclear lamins, diseases and aging. *Curr. Opin. Cell Biol.* **18**, 335-341.

Nigg, E. A., Kitten, G. T. and Vorburger, K. (1992). Targeting lamin proteins to the nuclear envelope: the role of CaaX box modifications. *Biochem. Soc. Trans.* **20**, 500-504.

Patrizi, G. and Poger, M. (1967). The ultrastructure of the nuclear periphery. The zonula nucleum limitans. *J. Ultrastruct. Res.* **17**, 127-136.

Prüfert, K., Vogel, A. and Krohne, G. (2004). The lamin CxxM motif promotes nuclear membrane growth. *J. Cell Sci.* **117**, 6105-6116.

Ralle, T., Grund, C., Franke, W. W. and Stick, R. (2004). Intranuclear membrane structure formations by CaaX-containing nuclear proteins. *J. Cell Sci.* **117**, 6095-6104.

Rowat, A. C., Foster, L. J., Nielsen, M. M., Weiss, A. M. and Ipsen, J. H. (2005). Characterization of the elastic properties of the nuclear envelope. *J. R. Soc. Interface* **2**, 63-69.

Sive, H. L., Grainger, R. M. and Harland, R. M. (2000). *Early Development of Xenopus laevis: A Laboratory Manual*. Cold Spring Harbor, NY: Cold Spring Harbor Laboratory Press.

Stewart, M. and Whytock, S. (1988). The structure and interactions of components of the nuclear envelopes from *Xenopus* oocyte germinal vesicles observed by heavy metal shadowing. *J. Cell Sci.* **90**, 409-423.

Stick, R. (1987). *Dynamics of the Nuclear Lamina During Mitosis and Meiosis*. New York: Academic Press.

Stick, R. (1988). cDNA cloning of the developmentally regulated lamin LIII of *Xenopus laevis*. *EMBO J.* **7**, 3189-3197.

Stick, R. (1992). The gene structure of *Xenopus* nuclear lamin A: a model for the evolution of A-type from B-type lamins by exon shuffling. *Chromosoma* **101**, 566-574.

Stick, R. and Krohne, G. (1982). Immunological localization of the major architectural protein associated with the nuclear envelope of the *Xenopus laevis* oocyte. *Exp. Cell Res.* **138**, 319-323.

Weber, K., Plessmann, U. and Traub, P. (1989). Maturation of nuclear lamin A involves a specific carboxy-terminal trimming, which removes the polyisoprenylation site from the precursor; implications for the structure of the nuclear lamina. *FEBS Lett.* **257**, 411-414.

Young, S. G., Fong, L. G. and Michaelis, S. (2005). Prelamin A, Zmpste24, misshapen cell nuclei, and progeria-new evidence suggesting that protein farnesylation could be important for disease pathogenesis. *J. Lipid Res.* **46**, 2531-2558.